

# Magnetostatics and the rotational sense of cycloidal spin spirals

N. Mikuszeit,<sup>1,\*</sup> S. Meckler,<sup>2</sup> R. Wiesendanger,<sup>2</sup> and R. Miranda<sup>1,3</sup>

<sup>1</sup>*Instituto Madrileño de Estudios Avanzados en Nanociencia, IMDEA-Nanociencia, Campus Universidad Autónoma de Madrid, ES-28049 Madrid, Spain*

<sup>2</sup>*Institute of Applied Physics, University of Hamburg Jungiusstr. 11, DE-20355 Hamburg, Germany*

<sup>3</sup>*Departamento de Física de la Materia Condensada and Instituto Nicolas Cabrera, Universidad Autónoma de Madrid, ES-28049 Madrid, Spain*

(Received 26 April 2011; published 2 August 2011)

The magnetostatic energy of a cycloidal spin-spiral configuration is calculated. The free-standing spiral is compared to the case of spirals that are brought in contact to a magnetically polarizable substrate. While a free-standing layer is energetically degenerate with respect to the spiral's sense of rotation, it is shown that a polarizable substrate breaks this symmetry and lifts the degeneracy. Consequently, a strongly polarizable substrate can stabilize (destabilize) a spin spiral that would be unstable (stable) without considering the magnetostatics of the substrate.

DOI: 10.1103/PhysRevB.84.054404

PACS number(s): 02.30.Em, 41.20.Gz, 75.10.-b

## I. INTRODUCTION

Homochiral spin-spiral configurations are observed in chiral crystals, such as MnSi<sup>1</sup> and Fe<sub>1-x</sub>Co<sub>x</sub>Si.<sup>2</sup> Below a critical temperature, these material systems show a phase transition from the paramagnetic phase to a helical phase. It was attributed to the Dzyaloshinskii-Moriya (DM) interaction,<sup>3,4</sup> which is a direct consequence of spin-orbit coupling in the presence of the broken inversion symmetry due to the chiral crystal structure. Alternatively, in multiferroic materials such as TbMnO<sub>3</sub> the inversion symmetry can be broken by electric fields,<sup>5</sup> which also gives rise to the formation of DM-driven spin spirals. Due to the lack of chirality in these crystals, the induced spiral configurations are of cycloidal instead of helical type but still possess a unique rotational sense. Only recently, homorotational magnetic cycloids could even be observed in magnetic thin-film systems, where the inversion symmetry is broken by the surface of otherwise inversion-symmetric crystals.<sup>6-8</sup> To date, there is a common agreement that the occurrence of spin spirals with a unique rotational sense is intimately related to the existence of a sufficiently strong antisymmetric interaction of DM type, whereas symmetric interactions of dipolar type do not favor one particular rotational sense.

In this article we discuss the magnetostatics of cycloidal spin spirals,<sup>8</sup> i.e., a continuous repetition of Néel-type walls<sup>9</sup> with a unique sense of rotation ( $\uparrow \rightarrow \downarrow \leftarrow \uparrow$ ). It is shown how the bare presence of a magnetically polarizable substrate—on purely magnetostatic grounds—breaks the symmetry to lift the degeneracy with respect to the spiral's sense of rotation. Hence, the common restriction to antisymmetric interactions must be dropped. On the other hand, one has to keep in mind that magnetostatic energy is not a driving force for the formation of cycloidal spin structures (a Néel-type structure creates volume charge) while a helical spin spiral, i.e., a continuous repetition of Bloch-type walls<sup>9</sup> ( $\uparrow \otimes \downarrow \odot \uparrow$ ), is volume-charge free and, therefore, has a lower magnetostatic energy.

For completeness, we will first review in Sec. II the results on a free-standing magnetic layer. In Sec. III, a polarizable substrate and its effect on the total magnetostatic energy will be considered.

## II. THE STRAY FIELD AND THE MAGNETOSTATIC SELF-ENERGY OF A CYCLOIDAL SPIN SPIRAL IN A FREE-STANDING LAYER

Due to symmetry the self-energy of a spin spiral—cycloidal or not—does not depend on the sense of rotation. To calculate the self-energy, it is required to calculate the stray field, including the demagnetizing field, first. The field  $\vec{H}$  is the negative gradient of the magnetic potential  $\Phi$ . The latter one is calculated using Fourier methods starting from a point dipole with moment  $\vec{m}$  and potential

$$\Phi_{\text{dip}} = -\frac{\vec{m}}{4\pi\mu_0} \cdot (\nabla|\vec{r}|^{-1}), \quad (1)$$

where  $\vec{r}$  is the coordinate relative to the dipole. Using the Fourier representation of  $|\vec{r}|^{-1}$ , at constant  $z$  the Fourier transform  $\hat{\Phi}_{\text{dip}}$  of the potential  $\Phi_{\text{dip}}$  of a point dipole reads<sup>10</sup>

$$\hat{\Phi}_{\text{dip}}(\vec{q}, z) = -\frac{e^{-2\pi|\vec{q}||z|}}{2\mu_0|\vec{q}|} [i\vec{q} \cdot \vec{m}_{\parallel} - \text{sgn}(z)|\vec{q}|m_z], \quad (2)$$

where  $\vec{m}_{\parallel} = (m_x, m_y)$  and  $\vec{q} = (q_x, q_y)$ . To consider a thickness  $h$ , one has to integrate  $\hat{\Phi}_{\text{dip}}(\vec{q}, z - \zeta)$  with respect to  $\zeta$  and the according limits; here, we choose the magnetic layer to be at  $-h \leq 2z \leq h$ . Note that in this case, we must replace the magnetic moment by a magnetic-moment line density such that the integration results in an extended magnetic moment. In case of a spin spiral in volume material, additional integration over the two-dimensional (2D) unit cell is required. Hence, in this case, one has to replace the point dipole moment by a magnetic-moment volume density, i.e., magnetization, such that the integration, again, results in a magnetic moment. In the following, this step has already been carried out and instead of the magnetic moment  $m$ , the magnetization  $M$  appears.

We restrict the spin spiral to the quasi-one-dimensional (1D) case with variations in  $x$  direction only, i.e.,  $M_x = M_S a(x)$  and  $M_z = M_S b(x)$ , where  $M_S$  is the saturation magnetization and the functions  $a$  and  $b$  naturally fulfill  $a^2(x) + b^2(x) = 1$  and have Fourier coefficients  $a_j$  and  $b_j$ ,

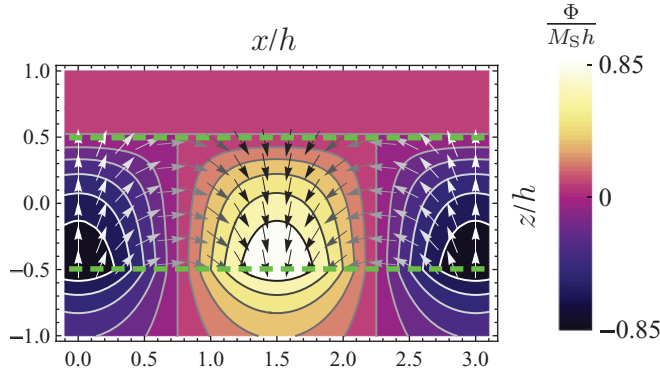


FIG. 1. (Color online) Magnetization vector field of a sinusoidal and cycloidal spin spiral. Contour lines give the constant magnetic potential. The magnetic layer is confined to  $2|z| \leq 1$ , which is also indicated by the dashed lines.

respectively. With  $q_j = j\lambda^{-1}$ ,  $j \in \mathbb{Z}$ , and the wavelength of the spiral  $\lambda$ , the potential  $\Phi_{ss}$  of the spin spiral has the form

$$\Phi_{ss}(\vec{r}) = -\frac{M_S}{2} \sum_{j \in \mathbb{Z}} e^{2\pi i q_j x} \times [ia_j \operatorname{sgn}(q_j) t(q_j, h, z) - b_j u(q_j, h, z)], \quad (3)$$

where  $t(q_j, h, z)$  is the integral of the exponential function in Eq. (2), while  $u(q_j, h, z)$  includes the additional sign function. Due to the modulus of  $z$ , the integral inside the layer differs from the outside solution and  $t$  and  $u$  read<sup>11</sup>

$$t(q_j, h, z) = \begin{cases} \frac{\sinh(\pi |q_j| h)}{\pi |q_j|} e^{-2\pi |q_j| z}, & |z| > \frac{h}{2}, \\ \frac{2 - e^{-\pi |q_j| (h+2z)} - e^{-\pi |q_j| (h-2z)}}{2\pi |q_j|}, & |z| \leq \frac{h}{2}, \end{cases} \quad (4)$$

and

$$u(q_j, h, z) = \begin{cases} \operatorname{sgn}(z) \frac{\sinh(\pi |q_j| h)}{\pi |q_j|} e^{-2\pi |q_j| z}, & |z| > \frac{h}{2}, \\ \frac{\sinh(2\pi |q_j| z)}{\pi |q_j|} e^{-\pi |q_j| h}, & |z| \leq \frac{h}{2}. \end{cases} \quad (5)$$

The 2D case can be treated in a similar way because all important integrals and derivatives appear in a similar way except the prefactors.<sup>12</sup>

As a 1D example, a sinusoidal spin spiral, i.e.,  $a_{\pm 1} = \pm(2i)^{-1}$  and  $b_{\pm 1} = 2^{-1}$  as well as its potential are shown in Fig. 1. Note that in the special case of a sinusoidal spiral, the potential is constant on one side of the magnetic layer, i.e., the stray field on this side is identical to zero, while it is nonzero on the other side. As mentioned before, we easily calculate the field by taking the negative gradient of the potential such that

$$H_x(h, x, z) = -\pi M_S \sum_{j \in \mathbb{Z}} e^{2\pi i q_j x} [a_j |q_j| t(q_j, h, z) + i q_j b_j u(q_j, h, z)] \quad (6)$$

and

$$H_z(h, x, z) = \frac{M_S}{2} \sum_{j \in \mathbb{Z}} e^{2\pi i q_j x} [ia_j \operatorname{sgn}(q_j) \tau(q_j, h, z) + b_j v(q_j, h, z)], \quad (7)$$

where

$$\tau(q_j, h, z) = \frac{d}{dz} t(q_j, h, z) = -2 \begin{cases} \operatorname{sgn}(z) \frac{\sinh(\pi |q_j| h)}{e^{2\pi |q_j| z}}, & |z| > \frac{h}{2}, \\ \frac{\sinh(2\pi |q_j| z)}{e^{\pi |q_j| h}}, & |z| \leq \frac{h}{2}, \end{cases} \quad (8)$$

and

$$v(q_j, h, z) = \frac{d}{dz} u(q_j, h, z) = 2 \begin{cases} -\frac{\sinh(\pi |q_j| h)}{e^{2\pi |q_j| z}}, & |z| > \frac{h}{2}, \\ \frac{\cosh(2\pi |q_j| z)}{e^{\pi |q_j| h}}, & |z| \leq \frac{h}{2}. \end{cases} \quad (9)$$

To finally get the energy density, we have to evaluate the integral

$$\mathcal{E} = -\frac{1}{\lambda h} \int_0^\lambda dx \int_{-\frac{h}{2}}^{\frac{h}{2}} dz \frac{\mu_0}{2} \vec{M} \cdot \vec{H}. \quad (10)$$

For symmetry reasons, which will be discussed in more detail below,  $M_x$  has a nonzero contribution only if interacting with the part of  $H_x$  that is proportional to  $a_j$ , whereas  $M_z$  has a nonzero contribution only if interacting with the part of  $H_z$  that is proportional to  $b_j$ . Therefore, we split the result into two parts, one due to  $M_x$ , i.e.  $\mathcal{E}^{(x)}$ , and one due to  $M_z$ , i.e.,  $\mathcal{E}^{(z)}$ . They read<sup>11</sup>

$$\mathcal{E}^{(x)} = \frac{\mu_0}{2} M_S^2 \sum_{j \in \mathbb{Z}} |a_j|^2 \left( 1 - \frac{1 - e^{-2\pi |q_j| h}}{2\pi |q_j| h} \right) \quad (11)$$

and<sup>13</sup>

$$\mathcal{E}^{(z)} = \frac{\mu_0}{2} M_S^2 \sum_{j \in \mathbb{Z}} |b_j|^2 \frac{1 - e^{-2\pi |q_j| h}}{2\pi |q_j| h}. \quad (12)$$

As the magnetostatic self-energy only depends on the modulus of  $a_j$  and  $b_j$ , naturally it does not depend on the sense of rotation of the spin spiral, which is encoded in the signs of  $a_j$  and  $b_j$ . Interestingly, in case of the sinusoidal spin spiral, the moduli of  $a_j$  and  $b_j$  are identical such that by adding Eqs. (11) and (12), the  $q_j$ -dependent fraction cancels out. Hence, the self-energy of a sinusoidal spin spiral in an infinite layer is always

$$\mathcal{E}_{\text{sinusoidal}} = \frac{\mu_0}{4} M_S^2, \quad (13)$$

which is independent of  $h$  and  $\lambda$ , and in contrast to sinusoidal helical spin spirals,<sup>14</sup> magnetostatics plays no role with respect to the equilibrium domain size.

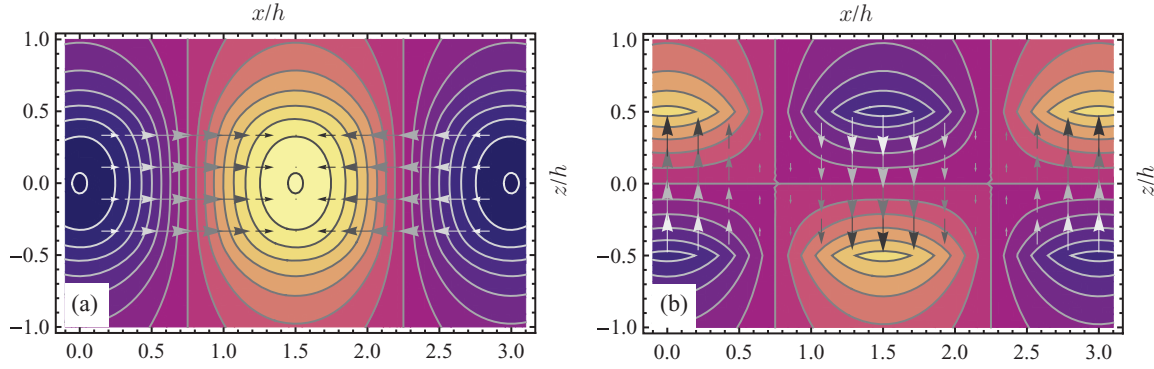


FIG. 2. (Color online) The potential of a sinusoidal cycloidal spin spiral as in Fig. 1 but decomposed into the contribution that originates from the  $x$  component of the magnetization (a) and the contribution due to the  $z$  component (b). The corresponding projections of the vector field are drawn on top. The color scale is the same as in Fig. 1.

### III. MAGNETOSTATIC ENERGY OF A CYCLOIDAL SPIN SPIRAL ON TOP OF A POLARIZABLE SUBSTRATE

While the self-energy of a free-standing cycloidal spin spiral does not depend on the sense of rotation, this changes if the magnetic layer is on top of a polarizable substrate. Naturally, we need a mechanism that breaks the symmetry to have an energy that depends on the sense of rotation. Here, the symmetry breaking is due to the presence of a polarizable substrate. From now on, we assume that the substrate occupies the half space at  $2z < -h$ .

The magnetic potential of the spin spiral can be decomposed into two parts: one is due to the  $x$  component and the other due to the  $z$  component of the magnetization. While the part of the potential due to  $M_x$  originates from volume charge, which is equally distributed along  $z$  and only varies along  $x$  [see Fig. 2(a)],  $M_z$  results in a surface charge that has odd parity upon reflection across the  $x$ - $y$  plane [see Fig. 2(b)]. Hence, the two parts have a different symmetry and the superposition leads to a nonsymmetric potential as can be seen in Fig. 1. As a consequence, the stray field for  $2z > h$  and  $2z < h$  is not identical. For the free-standing layer, this is not important, as on both sides there is vacuum, but in case of a substrate, the stray field to which this substrate is exposed depends on the sense of rotation of the spin spiral. If the substrate is polarizable, it will be polarized due to the stray field of the spin spiral. As the stray field depends on the sense of rotation so does the polarization of the substrate. The polarized substrate then also produces a stray field that naturally depends on the sense of rotation as well. This stray field changes the magnetostatic energy of the spin spiral such that we must conclude that in the presence of a polarizable substrate, the magnetostatic energy of a cycloidal spin spiral depends on the sense of rotation.

#### A. The stray field of a semi-infinite substrate, polarized by a spin spiral

Using Eqs. (6) and (7), we can calculate the stray field of the spin spiral inside the substrate. We further assume that the induced magnetization in the substrate is  $\vec{M}_{\text{ind}} = p\vec{H}$ , i.e., it is proportional to the field with polarizability  $p$  and  $|p| < 1$ . As a next step, we have to calculate the magnetic potential of the

substrate. It is possible to express the induced magnetization in the form

$$\begin{aligned}\vec{M}_{\text{ind}}(x, z) &= p\vec{H}(x, z) \\ &= pM_s \sum_{j \in \mathbb{Z}} e^{2\pi i q_j x} \begin{pmatrix} \alpha_j(h, z) \\ \beta_j(h, z) \end{pmatrix},\end{aligned}\quad (14)$$

where  $\alpha_j$  and  $\beta_j$  can be obtained by comparing Eqs. (14), (6), and (7). These are of course also the Fourier coefficients of the induced magnetization. The difference with the previous case is that the coefficients now depend on  $z$ . The induced magnetic potential of the substrate then reads

$$\begin{aligned}\Phi_{\text{ind}}(h, x, z) &= -\frac{pM_s}{2} \int_{-\infty}^{-\frac{h}{2}} d\zeta \sum_{j \in \mathbb{Z}} e^{2\pi i q_j x} e^{-2\pi |q_j z|} \\ &\quad \times [\alpha_j(h, \zeta) \text{sgn}(q_j) - \text{sgn}(z - \zeta) \beta_j(h, \zeta)] \\ &= p \frac{M_s}{2} \sum_{j \in \mathbb{Z}} e^{2\pi i q_j x} G(q_j, h, z) \\ &\quad \times [ia_j \text{sgn}(q_j) + b_j],\end{aligned}\quad (15)$$

where

$$G(q_j, h, z) = \frac{1 - e^{-2\pi |q_j| h}}{4\pi |q_j|} e^{-\pi |q_j| |h+2z|}. \quad (16)$$

The function  $G(q_j, h, z)$  is symmetric with respect to  $2z = -h$ , as the substrate only has a surface but not a volume charge. This is due to the fact that the magnetization vector field of the substrate is identical to the stray field of the spin spiral, which naturally has a zero divergence outside the magnetic layer, see Fig. 3(a).

The stray field of the substrate reads

$$H_{\text{ind},x}(h, x, z) = pM_s \sum_{j \in \mathbb{Z}} \pi e^{2\pi i q_j x} G(q_j, h, z) (a_j |q_j| - iq_j b_j) \quad (17)$$

and

$$H_{\text{ind},z}(h, x, z) = -p \frac{M_s}{2} \sum_{j \in \mathbb{Z}} e^{2\pi i q_j x} \gamma(q_j, h, z) (ia_j \text{sgn}(q_j) + b_j), \quad (18)$$

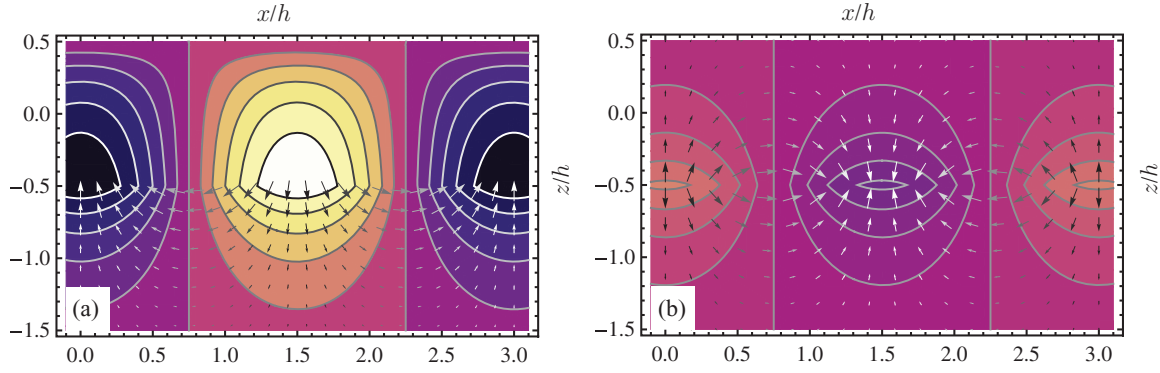


FIG. 3. (Color online) (a) Equipotential lines of the spin spiral as in Fig. 1. The vector field plotted on top is the stray field of the spiral that penetrates the substrate. Note, that this is—except from the factor  $p$ —equivalent to the induced magnetization in the substrate. (b) Potential due to the induced magnetization of the substrate. The vector field plotted on top is the corresponding stray field of the substrate. This field penetrates the spin spiral. The color scale in (b) is the same as in Fig. 1 when assuming the extreme case of a polarizability  $p = 1$ . Note, a smaller  $p$  will only change the scale, while the qualitative behavior stays the same.

where

$$\begin{aligned} \gamma(q_j, h, z) &= \frac{d}{dz} G(q_j, h, z) \\ &= \text{sgn}(h + 2z) \frac{e^{-2\pi|q_j|h} - 1}{2e^{\pi|q_j||h+2z|}}. \end{aligned} \quad (19)$$

Because the field  $\vec{H}_{\text{ind}}$  also exists in the region of the polarizable substrate [Fig. 3(b)], it actually modifies its polarization. Therefore, the exact solution for the polarization must be calculated self-consistently, e.g., by iterating the above steps until the solution converges. However, the  $n$ th-order iteration is of order  $p^n$ ; as  $p$  is usually significantly smaller than 1, these corrections are negligible.

### B. Magnetostatic energy of the spin spiral in the field of the substrate

To calculate the additional energy of the spin spiral in the field of the polarized substrate, one has to integrate

$$\mathcal{E}_{\text{ind}} = -\frac{1}{\lambda h} \int_0^\lambda dx \int_{-\frac{h}{2}}^{\frac{h}{2}} dz \mu_0 \vec{M} \cdot \vec{H}_{\text{ind}}. \quad (20)$$

As before, this integral will be split into two components: the contributions  $\mathcal{E}_{\text{ind}}^{(x)}$  due to  $M_x H_{\text{ind},x}$  and  $\mathcal{E}_{\text{ind}}^{(z)}$  due to  $M_z H_{\text{ind},z}$ , respectively. In detail they can be written as

$$\mathcal{E}_{\text{ind}}^{(x)} = -p \frac{\mu_0}{4} M_S^2 \sum_{j \in \mathbb{Z}} [|a_j|^2 - i \text{sgn}(q_j) a_j^* b_j] \frac{(1 - e^{-2\pi|q_j|h})^2}{2\pi|q_j|h} \quad (21)$$

and

$$\mathcal{E}_{\text{ind}}^{(z)} = -p \frac{\mu_0}{4} M_S^2 \sum_{j \in \mathbb{Z}} [i \text{sgn}(q_j) a_j b_j^* + |b_j|^2] \frac{(1 - e^{-2\pi|q_j|h})^2}{2\pi|q_j|h}, \quad (22)$$

where the asterisk denotes the complex conjugate. Combining Eqs. (21) and (22) and simplifying results in

$$\mathcal{E}_{\text{ind}} = -p \frac{\mu_0}{4} M_S^2 \sum_{j \in \mathbb{Z}} |i \text{sgn}(q_j) a_j + b_j|^2 \frac{(1 - e^{-2\pi|q_j|h})^2}{2\pi|q_j|h}. \quad (23)$$

This result reveals several important features. First, we note that there is no contribution for  $q = 0$  as the last fraction vanishes in the limit  $q \rightarrow 0$ . As any constant part ( $q = 0$ ) of the spin spiral does not produce a stray field outside the magnetic layer, it will, consequently, not polarize the substrate. Second, we see that if the substrate is paramagnetic, i.e.  $p > 0$ , the magnetostatic energy of the spin spiral is lowered as  $\mathcal{E}_{\text{ind}} \leq 0$ ,  $\forall p > 0$ . Finally, we note the peculiar dependency of  $\mathcal{E}_{\text{ind}}$  on the Fourier coefficients  $a_j$  and  $b_j$ . This combination reflects the dependency on the sense of rotation, as now the sign of  $a_j$  with respect to the sign of  $b_j$  becomes important. Let us consider, as an example, once again the sinusoidal spiral. The Fourier coefficients for the two possible sinusoidal spin spirals are given in Table I. Taking Fig. 2 into account, we see that at  $z < -0.5$  the potential due to the closest surface charges [see Fig. 2(b)] and the potential due to volume charges [see Fig. 2(a)] always have the same sign, i.e., at  $x/h = 0$  both show a negative minimum, at  $x/h = 0.75$  both become positive to reach their maxima at  $x/h = 1.5$ , etc. As a consequence the magnetic field is amplified on this side. On the other hand, at  $z > +0.5$  the potential due to the closest surface charge

TABLE I. Fourier coefficients for sinusoidal spin spirals. Depending on the signs of  $a_j$ , the substrate is on the side where the volume charge amplifies the magnetic field due to the surface charges (superscript a) or it diminishes it (superscript d) (see text). This changes the first factor of the sum in Eq. (23) (last two rows) and, therefore, the magnetostatic energy of the spin spiral. As in the case of a sinusoidal spin spiral, the stray field on the diminished side is zero and the corresponding factors (last row) are all identical zero.

$j$	$-1$	$1$
$q_j$	$-\frac{1}{\lambda}$	$\frac{1}{\lambda}$
$b_j$	$\frac{1}{2}$	$\frac{1}{2}$
$a_j^a$	$-\frac{1}{2i}$	$\frac{1}{2i}$
$a_j^d$	$\frac{1}{2i}$	$-\frac{1}{2i}$
$i \text{sgn}(q_j) a_j^a + b_j$	$1$	$1$
$i \text{sgn}(q_j) a_j^d + b_j$	$0$	$0$



has the opposite sign, such that the volume charge diminishes the total stray field. According to this, the first factor of the sum in Eq. (23) changes (see last two rows of Table I) and, consequently, the magnetostatic energy of the spin spiral.

### C. The magnetostatic self-energy of the substrate

As we consider the magnetostatic energy density of the spin spiral in the field of the substrate, it is also interesting to calculate the self-energy density of the substrate. As we did not calculate the field of the substrate self-consistently, this will only be a second-order correction to the total energy. Additionally, we have to take into account that the substrate is semi-infinite, where the field as well as the magnetization decay exponentially in  $z$  direction with a characteristic decay length of  $\lambda$ .<sup>15</sup> Hence, the volume energy density is zero. It is, however, possible to calculate the energy per unit area  $\epsilon_{\text{sub}}$ , i.e.,

$$\epsilon_{\text{sub}} = -\frac{1}{\lambda} \int_0^\lambda dx \int_{-\infty}^{-\frac{h}{2}} dz \frac{\mu_0}{2} \vec{M}_{\text{ind}} \cdot \vec{H}_{\text{ind}}. \quad (24)$$

Following the previous steps one eventually gets

$$\epsilon_{\text{sub}} = h \frac{\mu_0}{16} (p M_S)^2 \sum_{j \in \mathbb{Z}} |i \operatorname{sgn}(q_j) a_j + b_j|^2 \times \frac{(1 - e^{-2\pi |q_j| h})^2}{2\pi |q_j| h}. \quad (25)$$

The surface energy density of the substrate in Eq. (25) has many features in common with the energy volume density of Eq. (23), i.e., there is no contribution for  $q \rightarrow 0$  and it has the same dependency on the Fourier coefficients  $a_j$  and  $b_j$ . The additional volume density of the spin spiral can, however, be positive or negative, depending on the sign of the polarizability  $p$  of the substrate, whereas the magnetostatic self-energy of the substrate naturally must be positive; hence the  $p^2$  dependency. As mentioned before, this is a second-order correction and can be neglected for  $|p| \ll 1$ .

Finally, we note that by comparing the surface energy densities of the spin spiral and the substrate we have

$$|h \mathcal{E}_{\text{ind}}| > \epsilon_{\text{sub}}, \quad \forall_{\substack{p \neq 0 \\ |p| < 1}}, \quad (26)$$

such that a paramagnetic substrate will always lower the total magnetostatic energy. For  $p \in [-1, 1]$  the change in energy due to the polarizable substrate is a strictly decreasing function with respect to  $p$ . On the other hand, the last factor of Eq. (23) [and Eq. (25)] is zero for  $h \rightarrow 0$  and  $h \rightarrow \infty$ , such that it must present a maximum in the interval  $(0, \infty)$ . Hence, there is a ratio of  $h$  and  $\lambda$  that maximizes the gain in energy per unit area. In the presented first-order approximation, this ratio for the sinusoidal spin spiral reads

$$\frac{h}{\lambda} = -\frac{1 + 2W_{-1}\left(-\frac{1}{2\sqrt{e}}\right)}{4\pi} \approx 0.2, \quad (27)$$

where  $W_{-1}(z)$  is the lower branch of the Lambert- $W$  function.<sup>16</sup>

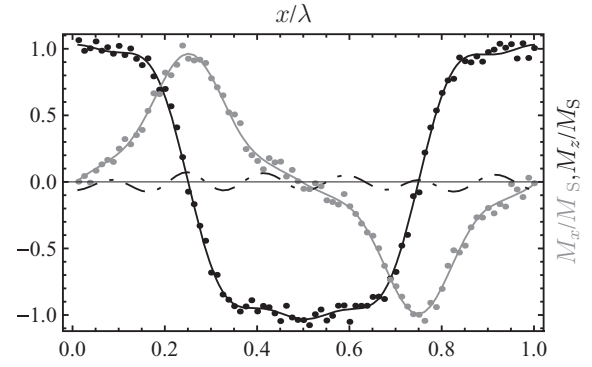


FIG. 4. Profile of a right-rotating spin spiral with  $\delta = 0.99$ . Magnetization component  $M_x$  is gray and  $M_z$  is black. The continuous lines show the Fourier approximation to the noisy data. The dashed line shows the relative deviation from  $M_x^2 + M_y^2 = M_S^2$ .

### IV. EXAMPLE CALCULATION FOR THE NONSINUSOIDAL CASE

In the previous chapters, the general solutions for the additional magnetostatic energy of a cycloidal spin spiral, due to a polarizable substrate, have been derived. The extreme case of a sinusoidal spiral, however, is only realized, for example, in the extreme case of dominant DM interaction. In general, the spiral profile is more complicated. Therefore, also an example for a nonideal case is given in the following.

Let us assume that the influence of the dipole-dipole interaction on the spiral profile is small, such that it alters only the total energy density. In this case, one can approximate the spiral profile, i.e., the rotation angle  $\varphi$  of the magnetization as a function of the position  $x$ , as<sup>17</sup>

$$\varphi(x) = \operatorname{am}\left(\frac{x}{\lambda x_0}, \delta\right), \quad (28)$$

where  $\operatorname{am}$  is the Jacobi amplitude,  $\delta$  a free parameter,<sup>18</sup> and

$$x_0 = 4E(\delta), \quad (29)$$

TABLE II. Fourier coefficients of a nonideal spin spiral (see Fig. 4) and the corresponding rotation-sensitive factor of Eq. (23). The additional minus sign at  $a_j$  in the last column corresponds to a left-rotating spiral, while the forth column represents a right-rotating spiral. The results are given with a precision of  $10^{-3}$ . Hence, within this precision, coefficients of order larger than five do not further affect the magnetostatic energy.

$j$	$10^3 a_j$	$10^3 b_j$	$ i \operatorname{sgn}(j) a_j + b_j ^2$	$ -i \operatorname{sgn}(j) a_j + b_j ^2$
-5	-1 + 30i	38 + i	$4 \times 10^{-3}$	0
-4	-5 + 3i	-1	0	0
-3	0	-118 + 2i	$14 \times 10^{-3}$	$14 \times 10^{-3}$
-2	0	-1	0	0
-1	-1 + 300i	595 + 2i	$801 \times 10^{-3}$	$87 \times 10^{-3}$
0	-2	5	0	0
1	-1 - 300i	595 - 2i	$801 \times 10^{-3}$	$87 \times 10^{-3}$
2	0	-1	0	0
3	0	-118 - 2i	$14 \times 10^{-3}$	$14 \times 10^{-3}$
4	-5 - 3i	-1	0	0
5	-1 - 30i	38 - i	$4 \times 10^{-3}$	0

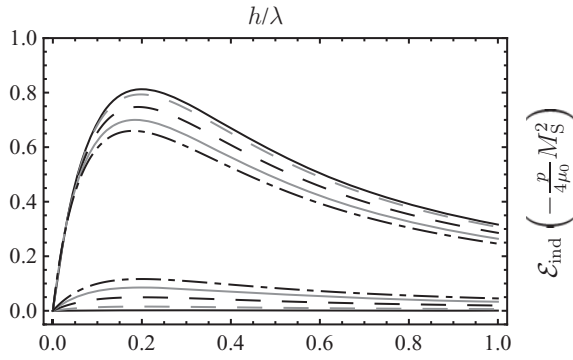


FIG. 5. Additional magnetostatic energy of the spin spiral due to the induced magnetization of the substrate. The upper branch is for right-rotating and the lower branch for left-rotating spirals. The parameter  $\delta$  varies as: 0.5 (black),  $10^{-1}$  (gray dashed),  $10^{-2}$  (black dashed),  $10^{-3}$  (gray), and  $10^{-4}$  (black dot-dashed).

where  $E$  is the complete elliptic integral of the second kind. For  $\delta < 0.5$ ,  $\varphi(x)$  is almost linear, resulting in an almost sinusoidal profile. In case of  $\delta \rightarrow 1$ , one obtains domains separated by walls that have almost the well-known arctan shape.

In Fig. 4 the case of  $\delta = 0.99$  is shown. Some data with noise have been simulated. The Fourier coefficients, presented in Table II are calculated from the data via numeric integration. The result of the integration, i.e., the Fourier approximation of the data, is shown as continuous lines. The dashed line represents the deviation from the requirement  $M_x^2 + M_y^2 = M_S^2$ , which has not been considered for the presented approximation. The small deviations from this condition are neglected in the following.

The last two columns of Table II present the rotation-sensitive factor of Eq. (23). The sum over these columns, weighted by the according factor of Eq. (23) with  $\lambda = 4.5 h$ , eventually gives

$$\begin{aligned} \mathcal{E}_{\text{ind}}^{\text{right}} &= -p \frac{\mu_0}{4} M_S^2 \times 0.657 \\ \mathcal{E}_{\text{ind}}^{\text{left}} &= -p \frac{\mu_0}{4} M_S^2 \times 0.077, \end{aligned} \quad (30)$$

In this case one still has a significant difference for right and left circular spin spiral. Furthermore, depending on the value of  $p$ , there can be a significant contribution from the induced polarization to the total magnetostatic energy.

Finally, calculations for different  $\delta$ , i.e., varying deviation from the perfect sinusoidal case, as a function of  $h/\lambda$  are shown in Fig. 5. With the chosen geometry (see previous paragraphs), the right-rotating spiral is always more strongly affected by the substrate. The previously calculated optimum wavelength of  $h/\lambda \approx 0.2$  only slightly changes to larger  $\lambda$  when  $\delta$

approaches 1. The important point, however, is that the changes with respect to  $\delta$  are small such that the sense of rotation can have a notable effect even for very inhomogeneous spin spirals. The influence of the induced magnetization vanishes for large  $\lambda$ , i.e.,  $h/\lambda \rightarrow 0$  in Fig. 5, as the volume charge density—one important component of the symmetry breaking—vanishes. It also disappears for  $\lambda \rightarrow 0$ , i.e.,  $h/\lambda \rightarrow \infty$ . This is due to the fact that the field of the induced magnetization decays exponentially into the spin spiral. As the characteristic decay length is given by  $\lambda$ , the volume fraction of the spiral that is affected by the field of the substrate decreases as  $\lambda/h$  decreases.

## V. CONCLUSIONS

The magnetostatic energy of a cycloidal spin spiral is independent of its sense of rotation only for a free-standing layer. A substrate with (sufficiently large) polarizability breaks this symmetry and lifts the magnetostatic energy degeneracy of right- and left-rotating spiral structures. In particular, this can play a role when some other mechanism, such as the Dzyaloshinskii-Moriya interaction,<sup>3,4</sup> can induce a cycloidal spin spiral. In this case, a strongly polarizable substrate can suppress or stabilize the spin spiral.

The effect vanishes for long as well as for extremely short spiral wavelengths. Because the effect is obviously wavelength dependent, one has also to conclude that it influences the equilibrium wavelength of the spin spiral.

In case of materials with rather weak magnetic polarizability, such as tungsten or platinum bulk crystals, the effect is negligible. However, it is known, e.g., for Co/Pt,<sup>19</sup> that the presence of magnetic surface layers can alter the electronic structure of these materials, therefore substantially increasing its polarizability in the interface region.

In the case of strongly paramagnetic substrates such as gadolinium, terbium,<sup>20</sup> or exotic materials like doped YbRh<sub>2</sub>Si<sub>2</sub>,<sup>21</sup> with magnetic susceptibilities of  $\chi_{\text{mol}} \approx 0.2 \text{ cm}^3/\text{mol}$  at room temperature and  $\chi_{\text{mol}} \approx 10^{-6} \text{ m}^3/\text{mol}$  around 1 K, respectively, the value of  $p$  can be on the order of 10%.<sup>22</sup> This value indicates that for appropriate material combinations and close to the transition between the collinear phase and the spin-spiral regime ( $D \approx D_c$ , cf. Refs. 17 and 23), the magnetostatic effects discussed in this article can have a strong impact on the formation of DM-driven surface spin spirals.

## ACKNOWLEDGMENTS

Funding by CONSOLIDER-INGENIO EN NANOCIENCIA MOLECULAR (ref. CSD2007 – 00010), by the Comunidad de Madrid through Project No. S2009/MAT-1726, and the Deutsche Forschungsgemeinschaft in the framework of SFB 668 is acknowledged.

\*nikolai.mikuszeit@imdea.org

<sup>1</sup>Y. Ishikawa, K. Tajima, D. Bloch, and M. Roth, *Solid State Commun.* **19**, 525 (1976).

<sup>2</sup>J. Beille, J. Voiron, and M. Roth, *Solid State Commun.* **47**, 399 (1983).

<sup>3</sup>I. Dzyaloshinsky, *J. Phys. Chem. Solids* **4**, 241 (1958).

- <sup>4</sup>T. Moriya, *Phys. Rev.* **120**, 91 (1960).
- <sup>5</sup>Y. Yamasaki, H. Sagayama, T. Goto, M. Matsuura, K. Hirota, T. Arima, and Y. Tokura, *Phys. Rev. Lett.* **98**, 147204 (2007).
- <sup>6</sup>M. Bode, M. Heide, K. von Bergmann, P. Ferriani, P. Heinze, G. Bihlmayer, A. Kubetzka, O. Pietzsch, S. Blügel, and R. Wiesendanger, *Nature (London)* **447**, 190 (2007).
- <sup>7</sup>P. Ferriani, K. von Bergmann, E. Y. Vedmedenko, S. Heinze, M. Bode, M. Heide, G. Bihlmayer, S. Blügel, and R. Wiesendanger, *Phys. Rev. Lett.* **101**, 027201 (2008).
- <sup>8</sup>S. Meckler, N. Mikuszeit, A. Pressler, E. Y. Vedmedenko, O. Pietzsch, and R. Wiesendanger, *Phys. Rev. Lett.* **103**, 157201 (2009).
- <sup>9</sup>S. Chikazumi, *Physics of Ferromagnetism* (Clarendon Press, Oxford, 1997).
- <sup>10</sup>R. J. Blakely, *Potential Theory in Gravity & Magnetic Applications* (Cambridge University Press, 1995).
- <sup>11</sup>E. Y. Tsymbal, *Appl. Phys. Lett.* **77**, 2740 (2000).
- <sup>12</sup>This is mainly due to the fact that in the 1D case,  $\frac{q_x}{|q|} = \frac{q}{|q|}$  can be simplified to  $\text{sgn}(q)$  ( $q \neq 0$ ) while in 2D it has the form  $\frac{q_x}{\sqrt{q_x^2 + q_y^2}}$ .
- <sup>13</sup>A. Hubert and R. Schäfer, *Magnetic Domains* (Springer, Berlin, 1998).
- <sup>14</sup>B. Kaplan and G. A. Gehring, *J. Magn. Magn. Mater.* **128**, 111 (1993).
- <sup>15</sup>R. L. Wallace, *Bell Syst. Tech. J.* **30**, 1145 (1951).
- <sup>16</sup>R. M. Corless, G. H. Gonnet, D. E. G. Hare, D. J. Jeffrey, and D. E. Knuth, *Adv. Comput. Math.* **5**, 329 (1996).
- <sup>17</sup>Y. A. Izyumov, *Sov. Phys. Usp.* **27**, 845 (1984).
- <sup>18</sup> $\delta \in [0, 1]$ , depends on the exchange stiffness, the strength of the uniaxial anisotropy, and the DM interaction.<sup>17</sup>
- <sup>19</sup>S. Stähler, G. Schütz, P. Fischer, M. Knülle, S. Rüegg, S. Parkin, H. Ebert, and W. B. Zeper, *J. Magn. Magn. Mater.* **121**, 234 (1993).
- <sup>20</sup>*Handbook of Chemistry and Physics*, edited by R. C. Weast, 68th ed. (CRC Press, Boca Raton, 1987).
- <sup>21</sup>S. Friedemann, T. Westerkamp, M. Brando, N. Oeschler, S. Wirth, P. Gegenwart, C. Krellner, C. Geibel, and F. Steglich, *Nat. Phys.* **5**, 465 (2009).
- <sup>22</sup>Note that these systems have been chosen only for their large susceptibility. Up to this date, no DM-driven spin spiral at room temperature has been reported nor is it clear whether the example systems have sufficiently large spin-orbit coupling—resulting in a sufficiently large DM interaction—to establish spin spirals.
- <sup>23</sup>M. Heide, G. Bihlmayer, and S. Blügel, *Phys. Rev. B* **78**, 140403(R) (2008).